Template-Assisted Fabrication of Free-Standing Nanorod Arrays of a Hole-Conducting Cross-Linked Triphenylamine Derivative: Toward Ordered Bulk-Heterojunction Solar Cells

Niko Haberkorn,[†] Jochen S. Gutmann,[‡,§] and Patrick Theato[†,*]

[†]Institute of Organic Chemistry, University of Mainz, Duesbergweg 10-14, 55099 Mainz, Germany, [‡]Institute of Physical Chemistry, University of Mainz, Welderweg 11, 55099, Mainz, Germany, and [§]Max-Planck-Institut für Polymerforschung, Ackermannweg 10, 55128 Mainz, Germany

ABSTRACT Free-standing nanorod arrays of a thermally cross-linked semiconducting triphenylamine were fabricated on conductive ITO/glass substrates *via* an anodic aluminum oxide (AAO) template-assisted approach. By using a solution wetting method combined with a subsequent thermal imprinting step to fill the nanoporous structure of the template with a cross-linkable triphenylamine derivative, a polymeric replication of the AAO was obtained after thermal curing and selective removal of the template. To obtain well-aligned and free-standing nanorod arrays, aggregation and collapse of the nanorods were prevented by optimizing their aspect ratio and applying a freeze-drying technique to remove the aqueous medium after the etching step. Because of their electrochemical properties and their resistance against organic solvents after curing, these high density nanorod arrays have potential application in organic photovoltaics.

KEYWORDS: triarylamine · semiconductive polymer(s) · template-assisted patterning · anodic aluminum oxide · nanorod(s) · organic photovoltaics

Arrays of nanometer-scale structures such as nanorods, nanowires, and nanotubes have attracted increasing attention, mainly because of the potential application in many fields of research like data storage,[1−3] artificial actuators,[4,5] surfaces exhibiting special wetting probabilities,[6−8] sensing,[9] and optoelectronics.[10−12] For example, one crucial and still very challenging part of the fabrication of high-efficient organic solar cells is to produce a nanometer-scale interpenetrating network of a donor and an acceptor phase, with an interfacial distance smaller than the exicton diffusion length (*ca.* 10−20 nm) in the organic material.[13] An ideal morphology that has been proposed for these cells consists of an array of vertically aligned hole-conducting polymeric nanorods attached to an electrode and surrounded by an electron-conducting material connected to a cathode or *vice versa*.[14,15]

Polymeric nanorods and nanowires can be fabricated by submicrolithography,[16] electro-spinning,[17] mechanical drawing,[18] and template-based methods.[19] For the production of highly ordered nanorod arrays the template-based approach seems to be the most suitable. Track-etched polymer membranes or block copolymer thin films as well as anodic aluminum oxide (AAO) membranes are widely used as templates to prepare nanowires. The former usually are made by bombarding a polycarbonate sheet with nuclear fission fragments to create damage tracks and then chemically etch these track into pores.[20] The membranes were used to fabricate arrays of conducting polymer rods but their pores are only randomly distributed and their areal density of $\sim 10^9$ pores/cm^2 is relatively low compared to other template-based methods.[21,22]

By using thin films of diblock copolymers with cylindrically aligned microdomains, porous templates with areal densities in excess of 10^{11} pores/cm^2 can be obtained after selective removal of the minor component of the block copolymer.[23−27] For example, Russell and co-workers recently showed the fabrication of nanorods of electropolymerized polypyrrole by using diblock copolymers templates of polystyrene-*block*-poly(methylmethacrylate).[28]

AAO membranes provide lateral pore densities comparable to that of block copolymer templates but they also allow a greater range of pore sizes (pore diameter and pore length) and offer a higher thermal

*Address correspondence to theato@uni-mainz.de.

Received for review March 2, 2009 and accepted May 13, 2009.

Published online May 19, 2009.
10.1021/nn900207a CCC: $40.75

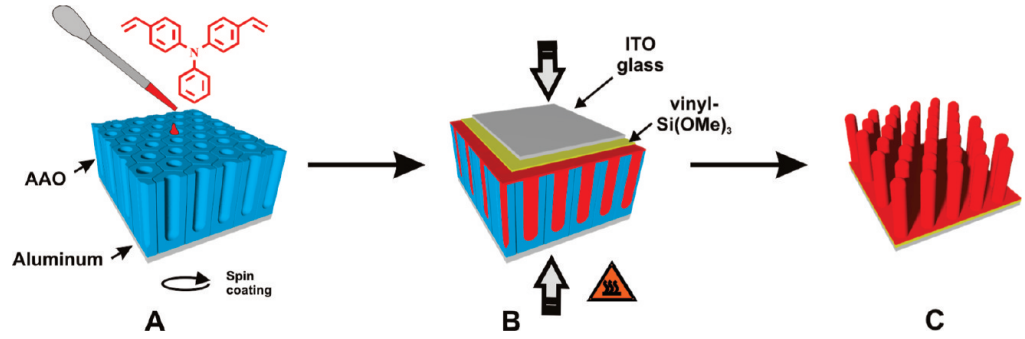

Scheme 1. Schematic diagram of the template-assisted fabrication of cross-linked free-standing nanorod arrays.

and mechanical stability. They can easily be fabricated by a controlled anodization process and have been well characterized in the last decades.[7,29−32] Polymeric nanorods and nanotubes have been fabricated by either wetting of the porous alumina template with (i) a polymer solution or (ii) a melt or by direct polymerization of a monomer inside of the template.[33] For example, the latter case has been used to prepare nanowires and nanotubes of polypyrrole, poly(3-methylthiophene) and poly(3,4-ethylenedioxythiophene) (PEDOT) by electropolymerization.[34−36] One very challenging step for the template-based fabrication of arrays of free-standing nanorods is the retention of the integrity of the polymeric structure after the selective removal of the template. The nanorods tend to collapse and lose their well-aligned orientation during the wet-chemical etching of the template in acidic or alkaline solutions. These collapsing and aggregation is mainly caused by capillary forces between the rods upon drying. Approaches to overcome aggregation mainly avoid the occurrence of liquid/solid interfaces during the removal of the template, for example by supercritical drying or non-wet-chemical mechanical release from the template.[37−39]

In this work, we describe the fabrication of arrays of high density free-standing nanorods composed of a cross-linked triphenylamine derivative on ITO/glass substrate by using AAO templates. Because of the limited usability of aggregated arrays in photovoltaic devices, one of the key issues is to overcome aggregation and collapsing of the semiconducting nanorods after removal of the template Therefore, the aspect ratio of the rods was varied by using AAO templates, whose pore length and diameter can be precisely controlled during their fabrication. We also demonstrate that the tendency of forming aggregates of nanorods can be significantly decreased by applying a freeze-drying step after wet-chemical etching of the porous alumina.

RESULTS AND DISCUSSION

The template-assisted fabrication of arrays of hole-conducting nanorods seems to be an appropriate approach for building up polymer/polymer solar cells with a well-defined photoactive layer consisting of nanorods embedded into an electron-conducting matrix. For the application in such photovoltaic devices the arrays of nanorods have to fulfill a number of requirements. First, the dimension of the rods needs to be adapted to the needs in organic photovoltaics. Owing to the relatively low exciton diffusion length in polymeric materials, the diameter and the space between the rods need to be in the order of several nanometers to provide a large donor/acceptor interface that is within the accessible exciton diffusion range. Furthermore the nanorods need to be contacted to a conducting electrode and have to be aligned perpendicular to

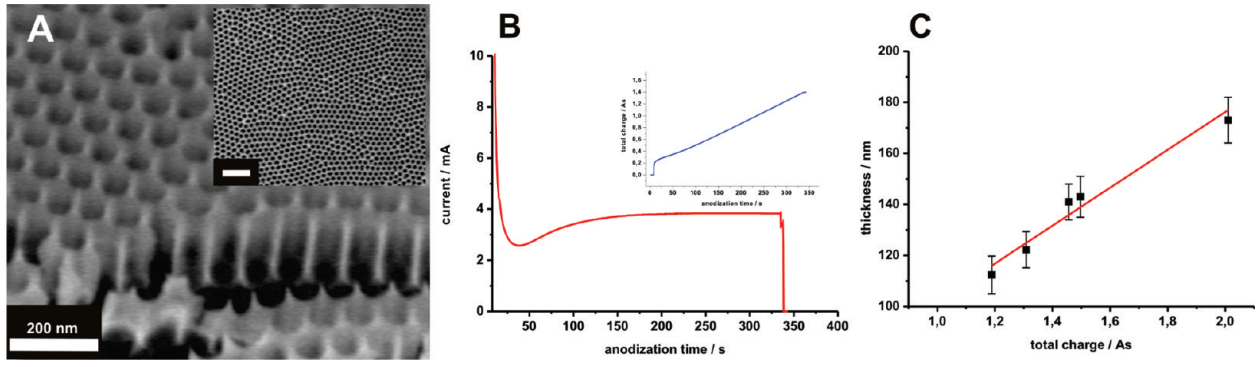

Figure 1. (A) Cross-sectional scanning electron microscopy (SEM) micrographs of an AAO template fabricated in 0.3 M oxalic acid of 2 °C at 40 V for 5.5 min. Pore widening was carried out in 5 wt % phosphoric acid at 25 °C for 35 min (inset: top view of the AAO; scale bar, 500 nm). (B) Corresponding current−time transient during the second anodization step of the aluminum substrate (inset: charge used for the anodization as a function of time). (C) Film thickness as a function of total charge used during the anodization step in 0.3 M oxalic acid of 2 °C at 40 V.

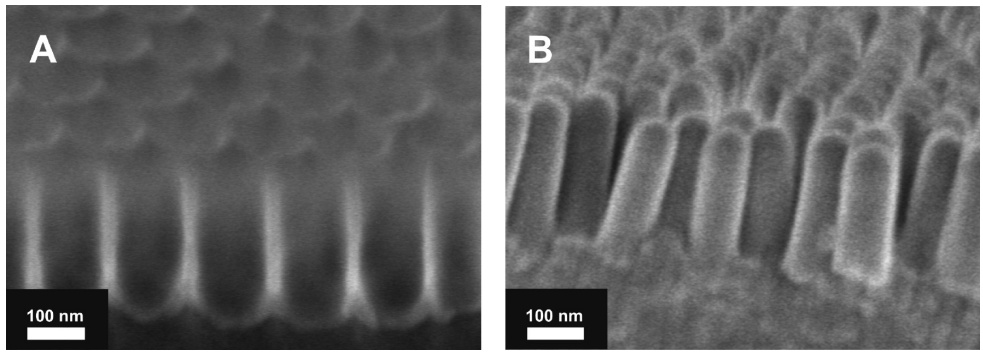

Figure 2. SEM images of (A) side view of an empty AAO template and (B) cross-section of the corresponding cross-linked DVTPA replica after removal of the AAO by treatment with a 0.9 M KOH solution (30 min, room temperature).

the substrate. To provide the maximal interfacial area and to permit a subsequent complete filling of the space between the rods with an electron-conducting material, it is crucial that the nanorods are free-standing and do not show any sign of aggregation and collapses. In addition, a high chemical resistance of the nanorod array against organic solvents is required for a subsequent spin-coating of the second polymer layer. We present a template-assisted approach, which allows the fabrication of large-area and high density arrays of nanorods fulfilling the criteria mentioned above. Scheme 1 illustrates the stepwise production of these arrays.

For the template-assisted patterning of the semiconducting triphenylamine derivative DVTPA, the use of AAO templates seemed to be promising since the parameters of their pores, such as diameter, pore-interdistance, and length can independently be varied during the fabrication process. As a consequence, this offers the possibility to exactly tune the structural properties of the nanorods replicating the structure of the AAO. The templates were fabricated by a well-established two step anodization process in oxalic acid yielding templates with an interpore distance of ~100 nm and pore diameters down to 40 nm. Pore lengths of only several hundreds of nanometers are desired for potential application in photovoltaics. These thin templates were fabricated by performing a short second anodization step for less than 10 min. The obtained thickness of AAO membranes usually correlates linearly with the anodization time when micrometer thick membranes are produced.[40] However, we observed that for thin templates a correlation between the pore length and the total charge used for the anodization seems to be a more suitable correlation parameter rather than the anodization time because of the typical variation of current density at the beginning of the pore formation. Furthermore, determination of the thickness by measuring the total charge instead of the time minimized the influences from experimental variations like temperature fluctuations.

Figure 1A shows a cross-sectional and a top view SEM micrograph of one AAO template anodized for 5.5 min at 40 V, demonstrating the determination of the pore lengths. Noteworthy, even after very short anodization times the pores are well-ordered and have a narrow size distribution. The total charge was determined by integration of the corresponding time/current transient, which is shown in Figure 1B exemplary for one of the anodization steps. A correlation curve (see Figure 1C) can be created by plotting the pore length of several AAO templates that have been anodized for different periods of time, ranging from 3 to 6 min, versus the total charge. With this correlation plot, it was possible to fabricate templates with very well adjusted pore lengths without checking every template by cross-sectional SEM, which usually requires the destruction of at least a small part of the template.

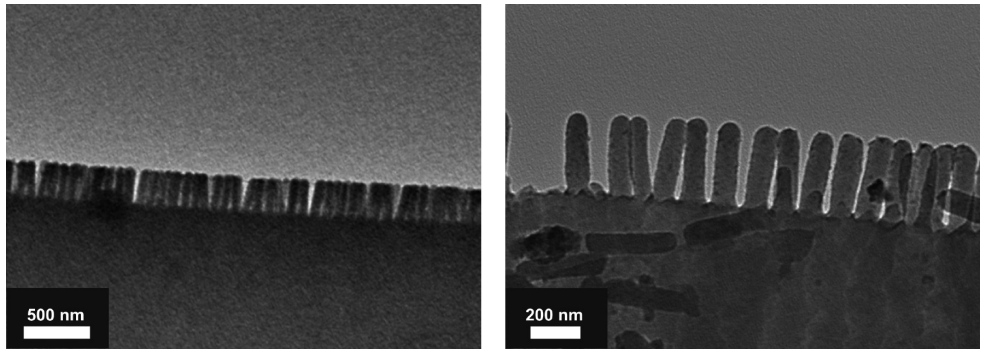

Figure 3. TEM cross sections of a cross-linked DVTPA replica after removal of the template. The patterned DVTPA film was detached from the ITO glass by dipping into liquid nitrogen and the mechanical stability was increased by coating of an epoxy film on the backside. After curing the sample was ultramicrotomed into 60 nm thick sections at room temperature.

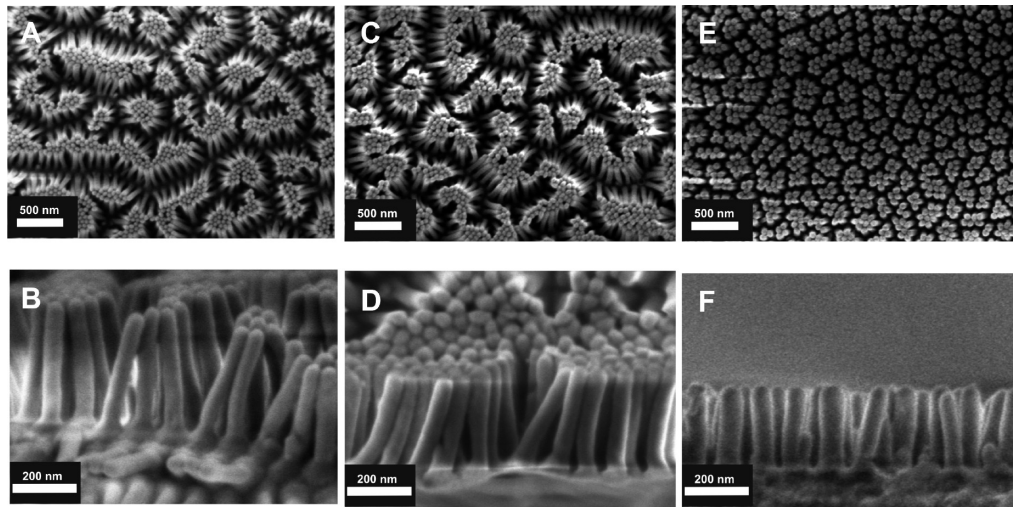

Figure 4. SEM images showing top and cross-sectional view of thermally cured DVTPA nanorod arrays after removal of the AAO template by treatment with a 4.5 M KOH solution (30 min, room temperature) followed by a conventional drying step: (A and B) nanorods with a length of 375 nm and a diameter of 60 nm (aspect ratio = 6.3, average interpore distance of the template 100 nm); (C and D) 310-nm long and 60-nm diameter nanorods (aspect ratio 5.2, average interpore distance of AAO, 100 nm); (E and F) nanopillars with an aspect ratio of 3.1 (length, 240 nm; diameter, 77 nm).

To obtain a complete filling of the fabricated AAO templates with the cross-linkable divinyltriphenylamine (DVTPA) and to attach this nanostructured material to an ITO/glass substrate, a solution wetting process combined with a subsequent thermal imprinting step was applied. In contrast to the wetting of hard templates with polymeric solutions, which usually results in the formation of hollow nanowires,[2] the wetting with solutions of small organic molecules, that is, DVTPA monomer, leads to formation of mechanically more stable, completely filled rods.

To minimize the thickness of the remaining DVTPA layer on top of the template after the solution wetting process, the solution was spin-coated on the AAO instead of drop-casted. After drying, an ITO/glass substrate that has been prefunctionalized with vinyltrimethoxysilane was pressed on the top of the filled AAO template and clamped together. The sample was ini-

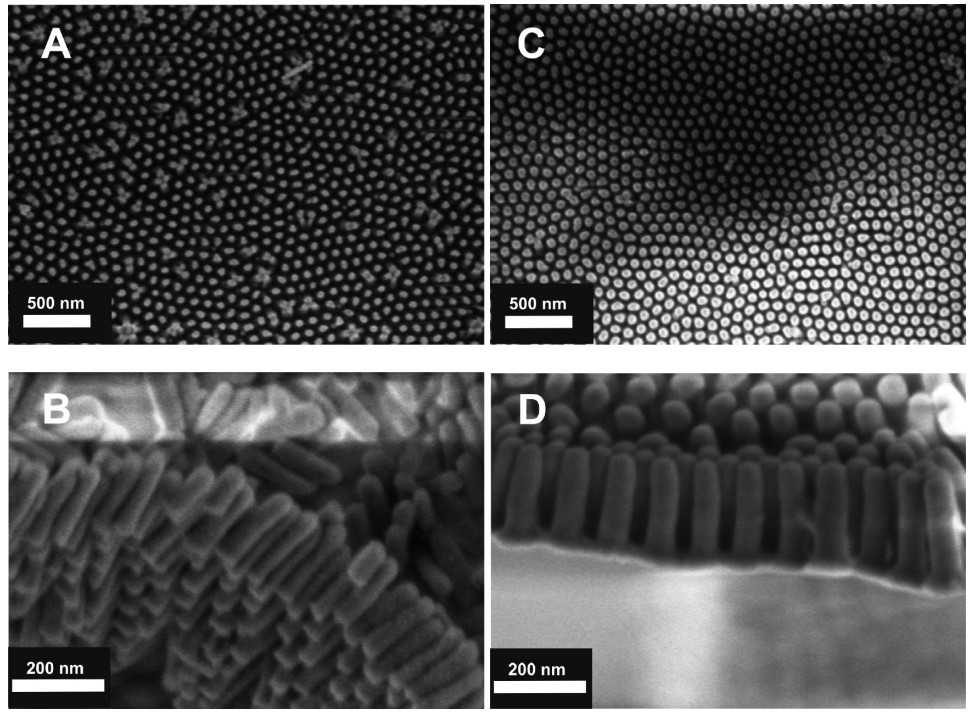

Figure 5. SEM micrographs of free-standing cross-linked DVTPA nanorod arrays after removal of the AAO template followed by a lyophilization step. Top (A) and cross-sectional (B) view of nanopillars with an aspect ratio of 4.0 (length, 200 nm; diameter, 50 nm). (C and D) Ensemble of nonaggregated nanorods with an aspect ratio of 3.1 (length, 200 nm; diameter, 65 nm).

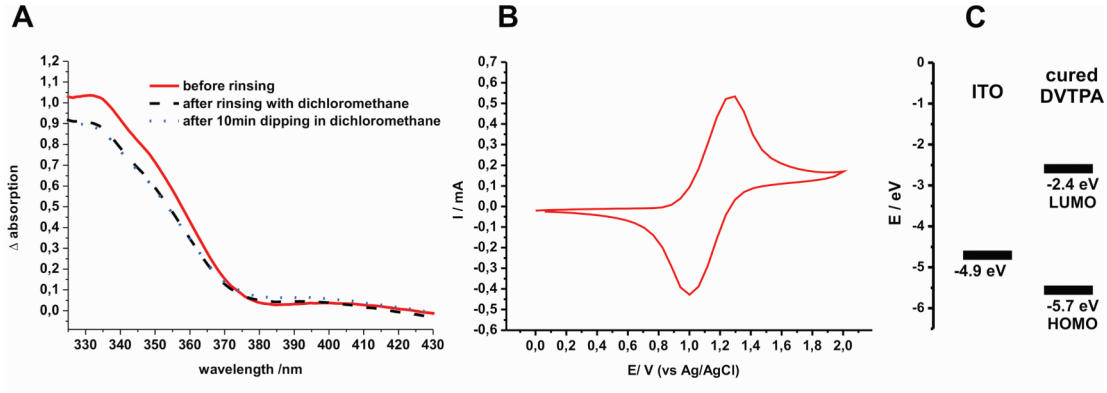

Figure 6. (A) Difference UV−vis absorption spectra of a spin-coated DVTPA film (10 wt % in dichloromethane, 3000 min^{-1}) on ITO glass cured at 150 °C for 1 h, before rinsing (solid line), after rinsing for three times with dichloromethane (dashed line) and after dipping for 10 min in dichloromethane (dotted line. (B) Cyclic voltammogram of a cured (2 h at 150 °C) patterned DVTPA film on ITO glass in a solution of *n*-Bu_4NPF_6 in acetonitrile (0.1 mol L^{-1}) at a scan rate of 0.1 V s^{-1}. (C) Energy level diagram for thermally cross-linked DVTPA. (HOMO level was converted from the measured oxidation potentials assuming the absolute energy level of ferrocene to be −4.8 eV; LUMO level was estimated from the HOMO level and energy gap, which was calculated from the onset of the UV−vis absorption spectrum.)

tially heated up *in vacuo* above the melting temperature of DVTPA (mp = 60 °C) to remove any air inclusions between the DVTPA film and the ITO/glass as well to improve the complete filling of the nanopores. Subsequently, the samples were thermally annealed at 150 °C for 180 min. Prior experiments have shown that using ITO substrates without any prefunctionalization resulted in a relatively low adhesion of the ITO substrate to the cured DVTPA film, which made it difficult to selectively remove the AAO and its supporting aluminum layer without causing any delamination of the patterned DVTPA film from the ITO/glass. The adhesion was dramatically increased by using ITO/glass that has been functionalized with vinyltrimethoxysilane as it provides a covalent attachment of the DVTPA film to the ITO *via* incorporating the vinyl group of the silane into the polymer network during thermal annealing procedure. Nevertheless, the layered construct was very fragile and delamination can occur during the removal of the template, in particular during wet chemical etching of the supporting aluminum because of the heat release during the exothermic reaction. Accordingly, the samples were ice-cooled during the chemical etching process and the concentration of the $CuCl_2$ solution, which was used to oxidatively etch the aluminum away, was lowered to 0.2 mol L^{-1} to slow down the exothermic reaction. As a result, pattered DVTPA films on ITO substrates could routinely be obtained.

Arrays of the polymeric nanorods (see Figure 2B) that match to the contours of the used AAO template (Figure 2A) can be obtained after subsequent removal of the AAO by treatment with KOH solution. To check if the fabricated nanorods were completely solid without any embedded gas bubbles or hollow canals, cross-sectional transmission electron microscopy (TEM) measurements were performed. The TEM images (see Figure 3) show a homogeneous filling of the rods, which ensures that they have a maximal mechanical stability and their conductivity is not degraded by any voids inside the material.

For the fabrication of free-standing nanorod arrays it is very important to overcome the collapsing and aggregation of the replica after removal of the template. Owing to their polymer nature, nanorods generally show a certain tendency to bend, and thus arrays of nanorods easily aggregate into bundles, which are mainly due to capillary forces acting on the rods during evaporation of the solvent after the wet-chemical etching step.[41,42]

To investigate the degree of aggregation as a function of the aspect ratio of the nanorods, arrays of cured DVTPA nanorods with aspect ratios ranging from 3.1 to 6.3 and lengths of 240−375 nm with a constant distance of 100 nm between the rods were fabricated. After wet-chemical removal of the AAO with KOH solution, the samples were conventionally air-dried. The top-view SEM micrographs of the samples are shown in the upper row of Figure 4.

Even though highly cross-linked poly(DVTPA) provides an improved mechanical stability, it can be seen that the regular patterns of the rods were distorted and bundles of rods have formed after the drying step. In the case of nanorods with an aspect ratio of 5.2 and higher (see Figure 4A,C) bundles consisting of more than 20 rods in average have formed. By reducing the aspect ratio down to 3.1, the degree of aggregation was decreased to an average of 6 rods per bundle but still the physical integrity of the arrays was distorted due to the capillary forces during the drying process.

Besides the influence of the aspect ratio and the mechanical stability of the rods the degree of aggregation also depends on the properties of the liquid that is used during the drying process. The capillary forces are proportional to the surface tension of the liquid and to the cosine of the contact angle at the liquid/rod interface. To minimize these forces either the contact angle must be brought close to 90° or the surface ten-

sion must be reduced. This can be achieved by either supercritical drying, which is an expensive process and demands special equipments, or by freeze-drying, a technique that has already been proven to be very useful in the area of lithography to prevent collapses of the resists by nullifying the surface tension.[43]

It turned out that the freeze-drying technique is indeed an appropriate and cost-effective method to minimize the aggregation of the cured DVTPA nanorods during the drying step. To remove residual water that remained on the top of the polymeric replica after the removal of the AAO by wet-chemical means, the samples were cooled down to −60 °C and dried *in vacuo*. Arrays of nanorods with an aspect ratio of up to 4.0 and a total length of 200 nm showed only a small degree of aggregation after the freeze-drying step (see Figure 5A). The majority of the rods were totally free-standing and nonaggregated. Applying the freeze-drying step to samples with an aspect ratio of the rods of 3.1 and a length of 200 nm proved that it was possible to totally suppress the aggregation and to obtain large areas of nonaggregated, free-standing nanorod arrays (Figure 5C). Thus, the preparation of nanopatterned films, which provide a large internal surface necessary for photovoltaic devices, has been achieved.

The thermally cured poly(DVTPA) films also showed a sufficient resistance against organic solvents, which would allow a subsequent polymer solution coating step. The thermal properties of monomeric DVTPA were studied by differential scanning calorimetry (DSC) measurements (see Supporting Information, Figure S1). The DSC measurement showed a broad exothermic transition in the range between 120 and 160 °C, corresponding to the heat released during of the cross-linking process. After an isothermal heating of DVTPA at 150 °C for 1 h and a slow cooling to room temperature, which are the same thermal conditions used for the curing step of the patterned DVTPA films, the rescan did not show any exothermic transition up to 180 °C, indicating that the cross-linking was completed during the first heating at 150 °C.

Further, the films on ITO/glass, which were thermally cured at 150 °C for 1 h under inert atmosphere, were washed thoroughly with dichloromethane, which is excellent solvent for the noncross-linked DVTPA, and the UV−vis spectra of the thin films before and after washing were investigated. After rinsing with dichloromethane, the absorption of the cured film slightly decreased (see Figure 6A). But even after dipping the film in dichloromethane for 10 min the absorption did not decrease further, which indicated that the cured films showed a sufficient resistance against organic solvents.

In the end, the highest occupied molecular orbital (HOMO) and lowest unoccupied molecular orbital (LUMO) energy levels of poly(DVTPA) were determined using cyclic voltammetry measurements along with UV−vis absorption spectroscopy. The HOMO level was determined from the oxidation peak of the cyclic voltammetry curve. Using E(ferrocene/ferrocene$^+$) = −4.8 eV below the vacuum level, the HOMO level was determined to be −5.7 eV for poly(DVTPA). The optical band gap value of 3.3 eV, obtained from the lower energy onset of the absorption spectra, was then used to calculate the LUMO level as −2.4 eV. Accordingly, the position of the energy levels and the totally reversible cyclic voltammetry of the arrays of the free-standing nanorods of poly(DVTPA) proved that the nanopatterned poly(DVTPA) films fulfill the required properties in order to be used as hole-conducting materials in an organic photovoltaic devices.

CONCLUSION

In this contribution, we reported on the fabrication of large arrays of semiconducting, polymeric nanorods attached to an ITO/glass electrode *via* an anodic aluminum oxide (AAO) template-assisted approach. The use of AAO templates with a dimensionally controllable, highly ordered porous structure allowed the production of polymeric nanorods with tunable aspect ratios. By filling the templates with a triphenylamine derivative *via* a template-wetting step combined with a subsequent imprinting, a good polymeric replication, which matches to the contours of the pores and does not show any voids, was obtained. The thermally initiated cross-linking of the triphenylamine derivative while pressing on an ITO/glass electrode, which was prefunctionalized with vinyltrimethoxysilane, resulted in good resistance against organic solvents and a sufficient adhesion between the substrate and the replica. Arrays of perfectly free-standing and nonaggregated nanorods with a length of 200 nm and an aspect ratio larger than 3 have been fabricated by applying a freeze-drying technique to remove the aqueous medium after the etching of the template. Because of the electrochemical properties and the highly ordered two-dimensional nanostructure, which provides a larger interface, these nanorod arrays have a potential application to build up ordered bulk-heterojunction solar cells.

EXPERIMENTAL SECTION

Materials. ITO-coated glass substrates (with sheet resistance of <10 Ohm/sq obtained from Präzisions Glas & Optik GmbH) were cleaned by ultrasonication in detergent, isopropyl alcohol, and acetone. They were then dried with a stream of pressurized N_2 and subjected to O_2 plasma cleaning for 10 min. For the silanization of ITO/glass substrates the O_2-plasma treated substrates were dipped into a 1 wt % solution of vinyltrimethoxysilane in tetrahydrofurane for 48 h at 40 °C.

Synthesis. Divinyltriphenylamine (DVTPA) was synthesized *via* a Vilsmeyer and a subsequent Wittig reaction starting from triphenylamine by modification of the procedure described in the lit-

erature.[44] The detailed synthetic procedure and characterization data are given in the Supporting Information.

Fabrication of AAO Templates. AAO templates were fabricated by a two-step anodization process developed by Masuda and Fukuda.[29,30] High purity aluminum (99.997%, 0.1 mm thick) purchased from Alfa Aesar was cleaned by sonification treatment in isopropyl alcohol and acetone, respectively, followed by an electropolishing step in a mixture of ethanol and perchloric acid (v/v 4:1) at a current density of 300−350 mA/cm^2 for 1 min at 0 °C. Subsequently the samples were rinsed with deionized water, isopropyl alcohol, and acetone. The anodization steps were performed in a self-build apparatus, similar to those described in the literature. Briefly, the aluminum sheets were mounted on a copper plate serving as the anode. A radial area of 2.27 cm^2 was exposed to an aqueous acidic solution. A platinum wire was used as the cathode. The apparatus was surrounded by a cryostatic bath to control the temperature during anodization and the electrolyte solution was rigorously stirred during anodization. The anodization current as a function of time was measured using a multimeter and recorded with an attached computer.

Anodization was performed in an aqueous solution of oxalic acid (c = 0.3 mol/L) at 40.0 V and 2 ± 1 °C. In the first step, aluminum was anodized for 6 h, followed by an etching step in aqueous solution of chromic acid (1.8 wt %) and phosphoric acid (6.0 wt %) at 60 °C for 12 h. The second anodization was performed for different time intervals ranging from 3 to 10 min. Pore widening was carried out in aqueous phosphoric acid (5 wt %) at 25 °C for a defined time.

Fabrication of Arrays of Free-Standing Nanorods. The template-assisted fabrication of arrays of free-standing nanorods is schematically shown in Scheme 1. The AAO templates consisted of an aluminum substrate with a thin porous anodized alumina layer with nanopores opened on one side. A solution of 4,4′-divinyltriphenylamine (DVTPA) in dichloromethane (20 wt %) was degassed by two freeze−pump−thaw cycles and subsequently spin-coated on the top of the AAO template (2000 rpm, 1 min). The samples were vacuum-treated for 30 min at room temperature. An ITO/glass substrate, which had been treated with O_2-plasma and silanized with vinyltrimethoxysilane, was pressed on the top of the spin-coated film and clamped together with the template. Under vacuum conditions the sample was heated up to 80 °C for 1 h and then cured for 3 h at 150 °C. Subsequently, the supporting aluminum layer was removed by treatment with a solution of $CuCl_2$ (c = 0.2 mol/L) at room temperature. By treatment with a solution of potassium hydroxide (5 wt %) for 1 h the porous alumina template was removed. The patterned polymer film attached to ITO/glass was rinsed with deionized water (Milliopore 18 MΩ) for several times and then stored in deionized water for 30 min to remove residual potassium and aluminum hydroxide. For samples that were not dried *via* freeze-drying technique, the water was removed under reduced pressure at room temperature. In the case of applying the freeze-drying technique, the wetted samples were first cooled down to −60 °C and then dried by subliming the ice under high vacuum conditions.

Characterization. The morphologies of the fabricated nanoporous AAO templates and their polymeric replicas were investigated by low voltage field emission scanning electron microscopy (FE-SEM, Zeiss LEO 1530) at 3 and 0.7 kV, respectively, without using any conductive coating. For cross-sectional TEM measurements a sample with a relatively thick (>1 μm) polymeric layer was fabricated in a similar way to the procedure described above by using drop-casting instead of spin-coating. Dipping the patterned polymer film into liquid nitrogen resulted in a delamination from the ITO/glass. The delaminated film was cut by ultramicrotomy, and TEM measurements were performed using a Philipps EM-420 at 120 kV. Cyclovoltametric measurements were performed using an Autolab PGSTAT30 (Eco Chemie) potentiosat/galvanostat. Pt wire and Ag/AgCl were used as the counter and reference electrode, respectively. The patterned hole-conducting polymer film on ITO/glass was used as the working electrode, and 0.1 M tetrabutylammonium tetrafluoroborate ($TBABF_4$) in acetonitrile was used as electrode.

Acknowledgment. N.H. gratefully acknowledges support of the international research and training group (IRTG 1404) funded by the DFG. The authors thank the department of Electron Microscopy at the Max-Planck Institute for Polymer Research in Mainz, in particular G. Glasser, providing support for SEM measurements.

Supporting Information Available: Experimental procedure and characterization of divinyltriphenylamine (DVTPA). This material is available free of charge *via* the Internet at http://pubs.acs.org.

REFERENCES AND NOTES

1. Martin, C. R. Nanomaterials: A Membrane-Based Synthetic Approach. *Science* **1994**, *266*, 1961–1966.
2. Steinhart, M.; Wehrspohn, R. B.; Gösele, U.; Wendorff, J. H. Nanotubes by Template Wetting: A Modular Assembly System. *Angew. Chem., Int. Ed.* **2004**, *43*, 1334–1344.
3. Mallet, J.; Yu-Zhang, K.; Mátéfi-Tempfli, S.; Mátéfi-Tempfli, M.; Piraux, L. Electrodeposited $L1_0Co_xPt_{1-x}$ Nanowires. *J. Phys. D: Appl. Phys.* **2005**, *38*, 909–914.
4. Berdichevsky, Y.; Lo, Y.-H. Polypyrrole Nanowire Actuators. *Adv. Mater.* **2006**, *18*, 122–125.
5. Shirota, Y.; Kageyama, H. Charge Carrier Transporting Molecular Materials and Their Applications in Devices. *Chem. Rev.* **2007**, *107*, 953–1010.
6. Lee, Y.; Park, S.-H.; Kim, K.-B.; Lee, J.-K. Fabrication of Hierarchical Structures on a Polymer Surface to Mimic Natural Superhydrophobic Surfaces. *Adv. Mater.* **2007**, *19*, 2330–2335.
7. Lee, W.; Jin, M.-K.; Yoo, W.-C.; Lee, J.-K. Nanostructuring of a Polymeric Substrate with Well-Defined Nanometer-Scale Topography and Tailored Surface Wettability. *Langmuir* **2004**, *20*, 7665–7669.
8. Cho, W. K.; Choi, I. S. Fabrication of Hairy Polymeric Films Inspired by Geckos: Wetting and High Adhesion Properties. *Adv. Funct. Mater.* **2008**, *18*, 1089–1096.
9. Martin, C. R. Template Synthesis of Electronically Conductive Polymer Nanostructures. *Acc. Chem. Res.* **1995**, *28*, 61–68.
10. Bai, R.; Ouyang, M.; Zhou, R.-J.; Shi, M.-M.; Wang, M.; Chen, H.-Z. Well-Defined Nanoarrays from an *n*-Type Organic Perylene−Diimide Derivative for Photoconductive Devices. *Nanotechnology* **2008**, *19*, 055604.
11. Xia, Y.; Yang, P.; Sun, Y.; Wu, Y.; Mayers, B.; Gates, B.; Yin, Y.; Kim, F.; Yan, H. One-Dimensional Nanostructures: Synthesis, Characterization, and Applications. *Adv. Mater.* **2003**, *15*, 353–389.
12. Musselman, K. P.; Mulholland, G. J.; Robinson, A. P.; Schmidt-Mende, L.; MacManus-Driscoll, J. L. Low-Temperature Synthesis of Large-Area, Free-Standing Nanorod Arrays on ITO/Glass and Other Conducting Substrates. *Adv. Mater.* **2008**, *20*, 4470–4475.
13. Yang, X.; Loos, J. Toward High-Performance Polymer Solar Cells: The Importance of Morphology Control. *Macromolecules* **2007**, *40*, 1353–1362.
14. Mayer, A. C.; Scully, S. R.; Hardin, B. E.; Rowell, M. W.; McGehee, M. D. Polymer-Based Solar Cells. *Mater. Today* **2007**, *10*, 28–33.
15. Gunes, S.; Neugebauer, H.; Sariciftci, N. S. Conjugated Polymer-Based Organic Solar Cells. *Chem. Rev.* **2007**, *107*, 1324–1338.
16. del Campo, A.; Arzt, E. Fabrication Approaches for Generating Complex Micro- and Nanopatterns on Polymeric Surfaces. *Chem. Rev.* **2008**, *108*, 911–945.
17. Greiner, A.; Wendorff, J. H. Electrospinning: A Fascinating Method for the Preparation of Ultrathin Fibers. *Angew. Chem., Int. Ed.* **2007**, *46*, 5670–5703.
18. Harfenist, S. A.; Cambron, S. D.; Nelson, E. W.; Berry, S. M.; Isham, A. W.; Crain, M. M.; Walsh, K. M.; Keynton, R. S.; Cohn, R. W. Direct Drawing of Suspended Filamentary Micro- and Nanostructures from Liquid Polymers. *Nano Lett.* **2004**, *4*, 1931–1937.

19. Cao, G.; Liu, D. Template-Based Synthesis of Nanorod, Nanowire, and Nanotube Arrays. *Adv. Colloid Interface Sci.* **2008**, *136*, 45–64.
20. Apel, P. Track Etching Technique in Membrane Technology. *Radiat. Meas.* **2001**, *34*, 559–566.
21. Martin, C. R. Membrane-Based Synthesis of Nanomaterials. *Chem. Mater.* **1996**, *8*, 1739–1746.
22. Parthasarathy, R. V.; Martin, C. R. Template-Synthesized Polyaniline Microtubules. *Chem. Mater.* **1994**, *6*, 1627–1632.
23. Park, C.; Yoon, J.; Thomas, E. L. Enabling Nanotechnology with Self Assembled Block Copolymer Patterns. *Polymer* **2003**, *44*, 6725–6760.
24. Thurn-Albrecht, T.; Schotter, J.; Kastle, G. A.; Emley, N.; Shibauchi, T.; Krusin-Elbaum, L.; Guarini, K.; Black, C. T.; Tuominen, M. T.; Russell, T. P. Ultrahigh-Density Nanowire Arrays Grown in Self-Assembled Diblock Copolymer Templates. *Science* **2000**, *290*, 2126–2129.
25. Crossland, E. J. W.; Ludwigs, S.; Hillmyer, M. A.; Steiner, U. Freestanding Nanowire Arrays from Soft-Etch Block Copolymer Templates. *Soft Matter* **2007**, *3*, 94–98.
26. Park, M.; Harrison, C.; Chaikin, P. M.; Register, R. A.; Adamson, D. H. Block Copolymer Lithography: Periodic Arrays of $\sim 10^{11}$ Holes in 1 Square Centimeter. *Science* **1997**, *276*, 1401–1404.
27. Tang, C.; Lennon, E. M.; Fredrickson, G. H.; Kramer, E. J.; Hawker, C. J. Evolution of Block Copolymer Lithography to Highly Ordered Square Arrays. *Science* **2008**, *322*, 429–432.
28. Lee, J.; Cho, S. H.; Park, S.-M.; Kim, J. K.; Kim, J. K.; Yu, J.-W.; Kim, Y. C.; Russell, T. P. Highly Aligned Ultrahigh Density Arrays of Conducting Polymer Nanorods using Block Copolymer Templates. *Nano Lett.* **2008**, *8*, 2315−2320.
29. Masuda, H.; Fukuda, K. Ordered Metal Nanohole Arrays Made by a Two-Step Replication of Honeycomb Structures of Anodic Alumina. *Science* **1995**, *268*, 1466–1468.
30. Masuda, H.; Yamada, H.; Satoh, M.; Asoh, H.; Nakao, M.; Tamamura, T. Highly Ordered Nanochannel-Array Architecture in Anodic Alumina. *Appl. Phys. Lett.* **1997**, *71*, 2770–2772.
31. Masuda, H.; Hasegwa, F.; Ono, S. Self-Ordering of Cell Arrangement of Anodic Porous Alumina Formed in Sulfuric Acid Solution. *J. Electrochem. Soc.* **1997**, *144*, L127−L130.
32. Nielsch, K.; Choi, J.; Schwirn, K.; Wehrspohn, R. B.; Gosele, U. Self-Ordering Regimes of Porous Alumina: The 10% Porosity Rule. *Nano Lett.* **2002**, *2*, 677–680.
33. Steinhart, M.; Wendorff, J. H.; Greiner, A.; Wehrspohn, R. B.; Nielsch, K.; Schilling, J.; Choi, J.; Gosele, U. Polymer Nanotubes by Wetting of Ordered Porous Templates. *Science* **2002**, *296*, 1997.
34. Demoustier-Champagne, S.; Stavaux, P.-Y. Effect of Electrolyte Concentration and Nature on the Morphology and the Electrical Properties of Electropolymerized Polypyrrole Nanotubules. *Chem. Mater.* **1999**, *11*, 829–834.
35. Park, D. H.; Kim, B. H.; Jang, M. G.; Bae, K. Y.; Joo, J. Characteristics and Photoluminescence of Nanotubes and Nanowires of Poly(3-methylthiophene). *Appl. Phys. Lett.* **2005**, *86*, 113116.
36. Cho, S. I.; Kwon, W. J.; Choi, S.-J.; Kim, P.; Park, S.-A.; Kim, J.; Son, S. J.; R., X.; Kim, S.-H.; Lee, S. B. Nanotube-Based Ultrafast Electrochromic Display. *Adv. Mater.* **2005**, *17*, 171–175.
37. Liang, Y.; Zhen, C.; Zou, D.; Xu, D. Preparation of Free-Standing Nanowire Arrays on Conductive Substrates. *J. Am. Chem. Soc.* **2004**, *126*, 16338–16339.
38. Grimm, S.; Schwirn, K.; Göring, P.; Knoll, H.; Miclea, P. T.; Greiner, A.; Wendorff, J. H.; Wehrspohn, R. B.; Gösele, U.; Steinhart, M. Nondestructive Mechanical Release of Ordered Polymer Microfiber Arrays from Porous Templates. *Small* **2007**, *3*, 993–1000.
39. Zhang, Y.; Lo, C.-W.; Taylor, J. A.; Yang, S. Replica Molding of High-Aspect-Ratio Polymeric Nanopillar Arrays with High Fidelity. *Langmuir* **2006**, *22*, 8595–8601.
40. Steinhart, M., Supramolecular Organization of Polymeric Materials in Nanoporous Hard Templates—Self-Assembled Nanomaterials II: Nanotubes. In *Advanced Polymer Science*; Shimazu, T., Ed.; Springer: Berlin, Heidelberg, 2008; pp 123−187.
41. Kondo, T.; Juodkazis, S.; Misawa, H. Reduction of Capillary Force for High-Aspect Ratio Nanofabrication. *Appl. Phys. A: Mater. Sci. Process.* **2005**, *81*, 1583–1586.
42. Tanaka, T.; Morigami, M.; Atoda, N. Mechanism of Resist Pattern Collapse during Development Process. *Jpn. J. Appl. Phys.* **1993**, *32*, 6059.
43. Tanaka, T.; Morigami, M.; Oizumi, H.; Ogawa, T. Freeze-Drying Process to Avoid Resist Pattern Collapse. *Jpn. J. Appl. Phys.* **1993**, *32*, 5813–5814.
44. Behl, M.; Hattemer, E.; Brehmer, M.; Zentel, R. Tailored Semiconducting Polymers: Living Radical Polymerization and NLO-Functionalization of Triphenylamines. *Macromol. Chem. Phys.* **2002**, *203*, 503–510.